

DNS of Interfacial Heat and Mass Transfer in Bubble Swarms

PRACEdays18

Néstor Balcázar^{2,1}, Óscar Antepara^{2,1}, Joaquim Rigola¹, Assensi
Oliva¹.

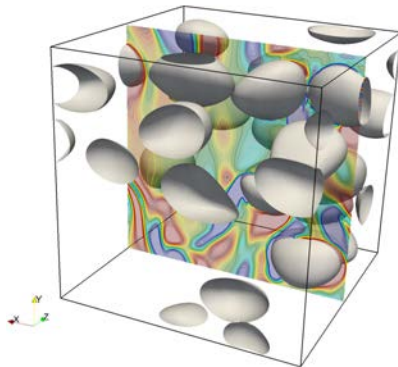
¹Heat and Mass Transfer Technological Centre (CTTC), Technical University of
Catalonia (UPC), <http://www.cttc.upc.edu/>, e-mail: nestor@cttc.upc.edu

²Termo Fluids, S.L., <http://www.termofluids.com/>, e-mail:
nestor@cttc.upc.edu, nestorbalcazar@yahoo.es

29 May 2018, Ljubljana-Slovenia.

Contents.

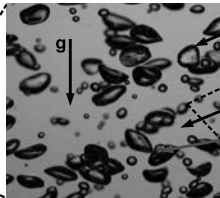
- 1 Introduction.
- 2 Mathematical formulation and numerical methods.
- 3 Numerical experiments.
- 4 Conclusions.



The objective of this work is to develop numerical methods for Direct Numerical Simulation (DNS) of bubbly flows with interfacial transport phenomena (variable surface tension, phase change, heat and mass transfer).

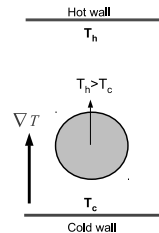
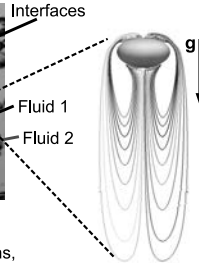
Introduction

- Bubbly flows with heat and mass transfer are important in natural processes and industrial applications:



Source: <http://www.iim.unam.mx/zenit/research.html>

Unit-operations in Chemical Engineering: Bubble columns, Chemical and Biochemical Bubble reactors, ...

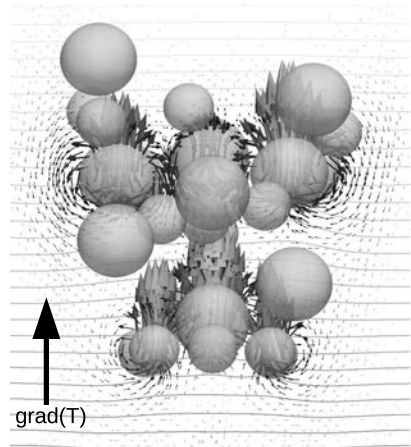


Thermocapillary flow:
Microgravity, microdevices.

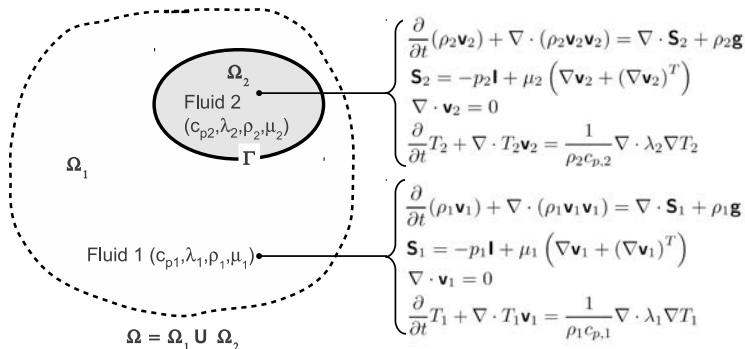
Assumptions considered in this work:

- **Incompressible** flows of two-phases (or two-fluid) with a clearly differentiated interface.
- **Newtonian** fluids.
- **No coalescence** of the fluid particles (bubbles, droplets).

- 1 Introduction.
- 2 **Mathematical formulation and numerical methods.**
- 3 Numerical experiments.
- 4 Conclusions.



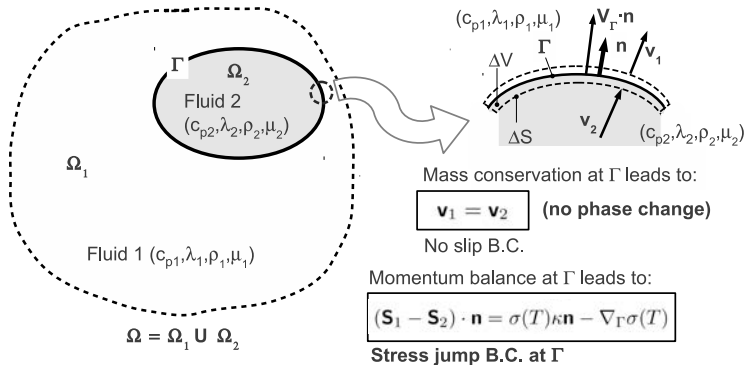
Navier-Stokes equations and energy equations^{1,2}



¹ Balcázar et al., (2014). A finite-volume/level-set method for simulating two-phase flows on unstructured grids, Int. J. Multiphase Flow 64, 55-72. <https://doi.org/10.1016/j.ijmultiphaseflow.2014.04.008>

² Balcázar et al., (2016). A level-set model for thermocapillary motion of deformable fluid particles, Int. J. Heat Fluid Flow 62, Part B, 324-343. <http://dx.doi.org/10.1016/j.ijheatfluidflow.2016.09.015>

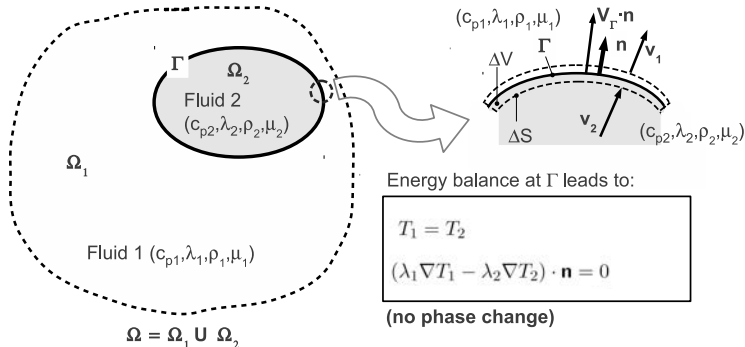
Boundary conditions at the interface



¹ Balcázar et al., (2014). A finite-volume/level-set method for simulating two-phase flows on unstructured grids, Int. J. Multiphase Flow 64, 55-72. <https://doi.org/10.1016/j.ijmultiphaseflow.2014.04.008>

² Balcázar et al., (2016). A level-set model for thermocapillary motion of deformable fluid particles, Int. J. Heat Fluid Flow 62, Part B, 324-343. <http://dx.doi.org/10.1016/j.ijheatfluidflow.2016.09.015>

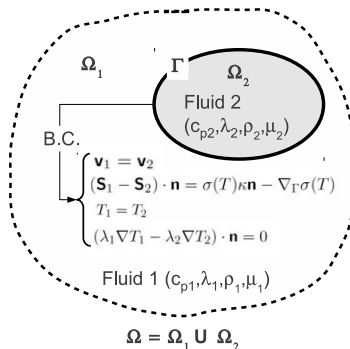
Boundary conditions at the interface



¹ Balcázar et al., (2014). A finite-volume/level-set method for simulating two-phase flows on unstructured grids, Int. J. Multiphase Flow 64, 55-72. <https://doi.org/10.1016/j.ijmultiphaseflow.2014.04.008>

² Balcázar et al., (2016). A level-set model for thermocapillary motion of deformable fluid particles, Int. J. Heat Fluid Flow 62, Part B, 324-343. <http://dx.doi.org/10.1016/j.ijheatfluidflow.2016.09.015>

Two-phase flow and energy equations: One marker model



$$\begin{aligned} \frac{\partial}{\partial t} \rho \mathbf{v} + \nabla \cdot \rho \mathbf{v} \mathbf{v} &= -\nabla p + \nabla \cdot \mu (\nabla \mathbf{v} + (\nabla \mathbf{v})^T) \dots \\ &\dots + \rho \mathbf{g} + (\sigma \kappa \mathbf{n} - \underbrace{\nabla \sigma + \mathbf{n}(\mathbf{n} \cdot \nabla) \sigma}_{\nabla_\Gamma \sigma}) \delta_\Gamma \\ \nabla \cdot \mathbf{v} &= 0 \\ \frac{\partial}{\partial t} T + \nabla \cdot T \mathbf{v} &= \frac{1}{\rho c_p} \nabla \cdot \lambda \nabla T \\ \beta &= \beta_1 H_1 + \beta_2 (1 - H_1) \quad \beta = \{\rho, \mu, \lambda, c_p\} \\ \sigma(T) &= \sigma_0 + \frac{d\sigma}{dT} (T - T_0) \end{aligned}$$

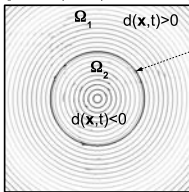
¹ Balcázar et al., (2014). A finite-volume/level-set method for simulating two-phase flows on unstructured grids, Int. J. Multiphase Flow 64, 55-72. <https://doi.org/10.1016/j.ijmultiphaseflow.2014.04.008>

² Balcázar et al., (2016). A level-set model for thermocapillary motion of deformable fluid particles, Int. J. Heat Fluid Flow 62, Part B, 324-343. <http://dx.doi.org/10.1016/j.ijheatfluidflow.2016.09.015>

Interface Capturing: Unstructured level-set method [1]

Standard level-set method

[Osher (1988), Sussman (1994)]

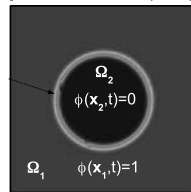


Interface
 $\Gamma(t) = \{x \mid d(x,t)=0\}$
 $\Gamma(t) = \{x \mid \phi(x,t)=0.5\}$

Signed distance function:
 $d(x,t) = \text{sign}(d) \min\{\|x - x_i\|\}$, Eq. (1)

Conservative level-set method

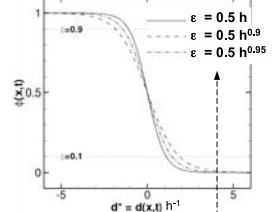
[Olsson and Kreiss (2005)]



Modified level-set function:

$$\phi(x,t) = \frac{1}{2} \left(\tanh \left(\frac{d(x,t)}{2\varepsilon} \right) + 1 \right) \quad \text{Eq. (2)}$$

Interface profile depends of ε



$$\varepsilon = 0.5 h^d$$

Geometrical properties of $\Gamma(t)$:

$$\mathbf{n} = \frac{\nabla \phi}{\|\nabla \phi\|} \quad \text{Eq. (3)}$$

Interface normals

$$\kappa(\phi) = -\nabla \cdot \mathbf{n} \quad \text{Eq. (4)}$$

Interface curvature

Physical properties, $\beta = \{\rho, \mu, \lambda\}$,

$$\beta(\phi) = \beta_1 \phi + \beta_2 (1 - \phi) \quad \text{Eq. (4)}$$

$$H_1 = \phi \quad \delta \Gamma = \|\nabla \phi\| \quad \text{Eq. (5)}$$

¹Balcázar et al., (2014). A finite-volume/level-set method for simulating two-phase flows on unstructured grids, Int. J. Multiphase Flow 64, 55-72. <https://doi.org/10.1016/j.ijmultiphaseflow.2014.04.008>

Interface Capturing: Unstructured level-set method [1]

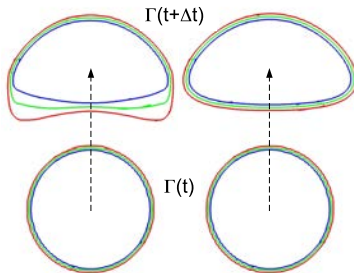


Fig. 1: Advection
Eq. 6

Fig. 2: Advection Eq. 6
+ Re-Initialization Eq. 7

$$\frac{\partial \phi}{\partial t} + \mathbf{v} \cdot \nabla \phi = 0$$

Advection equation
(no phase change)
Eq. 5

$$\nabla \cdot \mathbf{v} = 0$$

$$\frac{\partial \phi}{\partial t} + \nabla \cdot \phi \mathbf{v} = 0$$

Advection equation
in conservative form,
Eq. 6

$$\frac{\partial \phi}{\partial \tau} + \nabla \cdot \phi(1 - \phi) \mathbf{n}_{\tau=0} = \nabla \cdot \varepsilon \nabla \phi$$

Reinitialization equation, **Eq. 7**

¹Balcázar et al., (2014). A finite-volume/level-set method for simulating two-phase flows on unstructured grids, Int. J. Multiphase Flow 64, 55-72. <https://doi.org/10.1016/j.ijmultiphaseflow.2014.04.008>

Interface capturing: Coupled VOF/LS method[4]

Coupled volume-of-fluid/level-set method [4]: 1. Interface advection with geometrical VOF-PLIC

2. Surface tension by level-set method

1. Interface advection and geometrical reconstruction: VOF-PLIC method [3].

Indicator function,

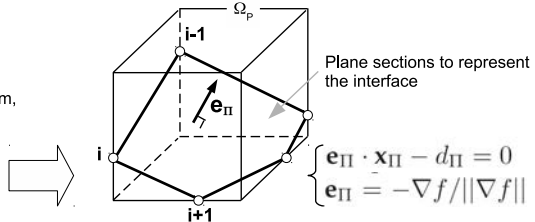
$$f(\mathbf{x}, t) = \begin{cases} 0 & \text{if } \mathbf{x} \in \Omega_1 \\ 1 & \text{if } \mathbf{x} \in \Omega_2 \end{cases}$$

Indicator function in discretized form,

$$f_P = \frac{\int_{\Omega_P} f(\mathbf{x}, t) dV}{\int_{\Omega_P} dV}$$

Advection equation,

$$\boxed{\frac{\partial f}{\partial t} + \mathbf{v} \cdot \nabla f = 0}$$



PLIC based on Young's reconstruction

³ Jofre, L., Lehmkuhl, O., Castro, J., Oliva, A., (2014). A 3-D Volume-of-Fluid advection method based on cell-vertex velocities, *Computers & Fluids* 94, 14-29.

⁴ Balcázar et al., (2016). A coupled volume-of-fluid/level-set method for simulation of two-phase flows on unstructured meshes, *Computers & Fluids* 124, 12-29.

<http://dx.doi.org/10.1016/j.compfluid.2015.10.005>

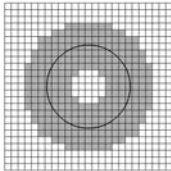
Interface capturing: Coupled VOF/LS method[4]

2. Distance function reconstruction [4] → Surface tension is computed using level-set method (signed distance function)

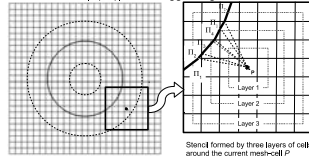
2.1. Initialize $d(\mathbf{x}, t)$

$$d(\mathbf{x}_P, t) = \begin{cases} d_{max} & \text{if } f(\mathbf{x}_P, t) \geq 0.5 \\ -d_{max} & \text{otherwise} \end{cases}$$

2.2. Detect a flagged region



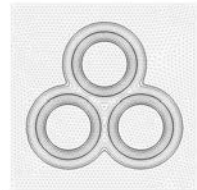
2.3. Calculate $|d(\mathbf{x}, t)|$ in the flagged region



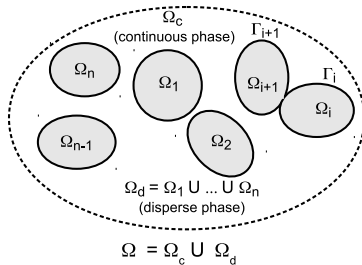
$$|d(\mathbf{x}_P, t)| = \min\{d_{P \rightarrow \Pi_1}^{min}, \dots, d_{P \rightarrow \Pi_i}^{min}, \dots, d_{P \rightarrow \Pi_n}^{min}\}$$

2.4. Calculate $d(\mathbf{x}, t)$

$$d(\mathbf{x}_P, 0) = \begin{cases} |d(\mathbf{x}_P, t)| & \text{if } f(\mathbf{x}_P, t) \leq 0.5 \\ -|d(\mathbf{x}_P, t)| & \text{otherwise} \end{cases}$$



Interface capturing: multiple marker CLS method [2, 5]



Regularization of physical properties [2,5]:

$$\beta = \{\rho, \mu, \lambda, c_p\}$$

$$\beta = \beta_d \phi_d + \beta_c (1 - \phi_d)$$

$$\phi_d(\mathbf{x}, t) = \max\{\phi_1(\mathbf{x}, t), \dots, \phi_{n_d-1}(\mathbf{x}, t), \phi_{n_d}(\mathbf{x}, t)\}$$

Interface advection and reinitialization [2,5]:

$$\left. \begin{aligned} \frac{\partial \phi_i}{\partial t} + \nabla \cdot \phi_i \mathbf{v} &= 0 \\ \frac{\partial \phi_i}{\partial \tau} + \nabla \cdot \phi_i (1 - \phi_i) \mathbf{n}_i &= \nabla \cdot \varepsilon \nabla \phi_i \end{aligned} \right\} \text{ for } i=1, \dots, n_d$$

Interface geometric properties [2,5]:

$$\left. \begin{aligned} \mathbf{n}_i(\phi_i) &= \frac{\nabla \phi_i}{\|\nabla \phi_i\|} \\ \kappa_i(\phi_i) &= -\nabla \cdot \mathbf{n}_i \end{aligned} \right\} \text{ for } i=1, \dots, n_d$$

Surface tension computed by CSF model (Brackbill et al. 1992).
 Extension to multiple marker CLS method in [2,5]:

$$\mathbf{f}_\sigma = \sum_{i=1}^{n_d} (\sigma(T) \kappa_i \mathbf{n}_i - \nabla \Gamma \sigma) \|\nabla \phi_i\|$$

The diagram shows two overlapping circles representing fluid particles Ω_i and Ω_{i+1} . A triangle is drawn with vertices at the centers of the circles and one vertex on the interface. This triangle represents the surface tension force acting on the interface.

² Balcázar et al., (2016). A level-set model for thermocapillary motion of deformable fluid particles, Int. J. Heat Fluid Flow 62, Part B, 324-343. <http://dx.doi.org/10.1016/j.ijheatfluidflow.2016.09.015>

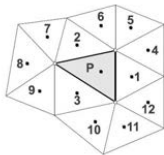
⁵ Balcázar et al., (2015). A multiple marker level-set method for simulation of deformable fluid particles, Int. J. Multiphase Flow 74, 125-142. <https://doi.org/10.1016/j.ijmultiphaseflow.2015.04.009>

Numerical methods: Discretization [1, 2]

- Finite-volume method for space discretization [1,2].
- Collocated grid arrangement.

General transport equation, Eq. 1

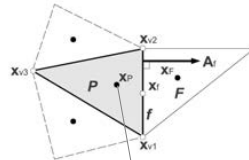
$$\underbrace{\int_{V_P} \frac{\partial \xi \psi}{\partial t} dV}_{\text{Accumulation}} = \underbrace{\oint_{A_P} (-\xi G^e(\psi) \mathbf{c} + \lambda \nabla \psi) \cdot d\mathbf{A}}_{\text{Convection Compression}} + \underbrace{\int_{V_P} S_\psi dV}_{\text{Diffusion Source}}$$



- Gradient at cell P :

$$(\nabla \psi)_P = (\mathbf{M}^T \mathbf{M})^{-1} \mathbf{M}^T \mathbf{Y}$$

Least-squares method, Eq. 2



$\{p, \mathbf{v}, \rho, \lambda, C_p, \mu, \phi\}$ in cell centroids

- Diffusion terms: Central-Difference Scheme.
- Convection terms: Novel unstructured flux limiters schemes [1,2].
- Pressure-velocity coupling: Fractional step method (Chorin, 1967).
- TVD Runge Kutta method for CLS equations.

¹ Balcázar et al., (2014). A finite-volume/level-set method for simulating two-phase flows on unstructured grids, Int. J. Multiphase Flow 64, 55-72. <https://doi.org/10.1016/j.ijmultiphaseflow.2014.04.008>

² Balcázar et al., (2016). A level-set model for thermocapillary motion of deformable fluid particles, Int. J. Heat Fluid Flow 62, Part B, 324-343. <http://dx.doi.org/10.1016/j.ijheatfluidflow.2016.09.015>

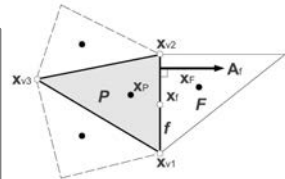
Numerical methods: Spatial discretization [2, 5]

- Finite-volume method on collocated grids for space discretization [1,2].

General transport equation, **Eq. 1**

$$\underbrace{\int_{V_P} \frac{\partial \xi \psi}{\partial t} dV}_{\text{Accumulation}} = \underbrace{\oint_{A_P} (-\xi G^e(\psi) \mathbf{c} + \lambda \nabla \psi) \cdot d\mathbf{A}}_{\text{Diffusion}} + \underbrace{\int_{V_P} S_\psi dV}_{\text{Source}}$$

Convection
Compression



$$\oint_{A_P} \lambda \nabla \psi \cdot d\mathbf{A} \approx \sum_f \lambda_f (\nabla \psi)_f = \sum_f \lambda_f \| \mathbf{A}_f \| \left(\underbrace{\left(\frac{\psi_F - \psi_P}{\| \Delta \mathbf{x}_{P-F} \|} \right)}_{\text{normal diffusion}} + (\nabla \psi)_f \cdot \underbrace{\left(\frac{\mathbf{A}_f}{\| \mathbf{A}_f \|} - \frac{\Delta \mathbf{x}_{P-F}}{\| \Delta \mathbf{x}_{P-F} \|} \right)}_{\text{transverse diffusion}} \right) \quad \text{Eq. 4}$$

- CD scheme

normal
diffusion

transverse
diffusion

¹ Balcázar et al., (2014). A finite-volume/level-set method for simulating two-phase flows on unstructured grids, Int. J. Multiphase Flow 64, 55-72. <https://doi.org/10.1016/j.ijmultiphaseflow.2014.04.008>

² Balcázar et al., (2016). A level-set model for thermocapillary motion of deformable fluid particles, Int. J. Heat Fluid Flow 62, Part B, 324-343. <http://dx.doi.org/10.1016/j.ijheatfluidflow.2016.09.015>

Numerical method: Spatial discretization [1, 2]

General transport equation, Eq. 1

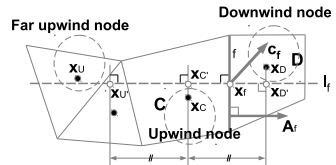
$$\underbrace{\int_{V_P} \frac{\partial \xi \psi}{\partial t} dV}_{\text{Accumulation}} = \underbrace{\oint_{A_P} (-\xi G^c(\psi) \mathbf{c} + \lambda \nabla \psi) \cdot d\mathbf{A}}_{\text{Convection Compression}} + \underbrace{\int_{V_P} S_\psi dV}_{\text{Source}}$$

Diffusion

$$\begin{aligned} \oint_{A_P} \xi G^c(\psi) \mathbf{c} \cdot d\mathbf{A}_P &\approx \sum_f G^c(\psi_f) \xi_f U_f^c \\ &= \sum_f \left[[\xi_f U_f^c, 0] G^c(\psi_{C'}) - [[-\xi_f U_f^c, 0] G^c(\psi_{D'}) \right] \\ &\quad + \frac{1}{2} \xi_f U_f^c L(\theta_f) (G^c(\psi_{D'}) - G^c(\psi_{C'})) \\ &= \text{upwind term} + \text{flux limiter term} \end{aligned}$$

Novel and accurate flux-limiter schemes on unstructured meshes [1,2].

Node-stencil:



- SUPERBEE (Momentum Eq.)
- SUPERBEE (Energy Eq.)
- SUPERBEE (Advection Eq.)
- CD (Reinit. Eq.)

¹ Balcázar et al., (2014). A finite-volume/level-set method for simulating two-phase flows on unstructured grids, Int. J. Multiphase Flow 64, 55-72. <https://doi.org/10.1016/j.ijmultiphaseflow.2014.04.008>

² Balcázar et al., (2016). A level-set model for thermocapillary motion of deformable fluid particles, Int. J. Heat Fluid Flow 62, Part B, 324-343. <http://dx.doi.org/10.1016/j.ijheatfluidflow.2016.09.015>

Numerical methods: Global algorithm [1, 2, 6]

Global algorithm for two-phase flows with variable surface tension [1,2,6]:

1. Initialize \mathbf{v} , T , κ_i , n_i , physical properties.

$$2. \Delta t = 0.1 \min \left(\frac{h}{\|\mathbf{v}\|}, \frac{\rho h^2}{\mu}, \left(\frac{h}{\|\mathbf{g}\|} \right)^{1/2}, h^{3/2} \left(\frac{\rho_1 + \rho_2}{4\pi\sigma} \right)^{1/2} \right)$$

3. Interface advection for $\phi_1, \dots, \phi_i, \phi_{i+1}, \phi_{nd}$ [1,2,6]

4. CLS re-initialization for $\phi_1, \dots, \phi_i, \phi_{i+1}, \phi_{nd}$ [1,2,6]

5. Calculate the global level-set function, $\phi_d(\mathbf{x}_p, t)$ [1,2,6]

6. Update physical properties, interface normals and curvature:

- $\kappa_i(\mathbf{x}_p, t)$, $\mathbf{n}_i(\mathbf{x}_p, t)$,
- $\rho(\mathbf{x}_p, t) = \rho(\phi_d)$, $\mu(\mathbf{x}_p, t) = \mu(\phi_d)$, $\lambda(\mathbf{x}_p, t) = \lambda(\phi_d)$,
- $c_p(\mathbf{x}_p, t) = c_p(\phi_d)$.

6. Solve energy equation and update $\sigma = \sigma(T)$ [1,2,6]

7. Solve momentum equation [1,2,6]

$$\frac{\rho \mathbf{v}^* - \rho^n \mathbf{v}^n}{\Delta t} = -\mathbf{C}^n + \mathbf{D}^n + (\rho - \rho_0) \mathbf{g} + \dots$$

$$\dots \sum_{i=1}^{n_d} (\sigma(T) \kappa_i(\phi_i) \mathbf{n}_i - \nabla_h \sigma(T) + \mathbf{n}_i (\mathbf{n}_i \cdot \nabla_h) \sigma(T)) || \nabla_h \phi_i ||$$

$$\nabla_h \cdot \left(\frac{1}{\rho} \nabla_h p \right) = \frac{1}{\Delta t} \nabla_h \cdot (\mathbf{v}^*) \quad \mathbf{e}_{\partial\Omega} \cdot \nabla_h p|_{\partial\Omega} = 0$$

$$\frac{\rho \mathbf{v} - \rho \mathbf{v}^*}{\Delta t} = -\nabla_h(p)$$

$$\mathbf{v}_f = \sum_{q \in \{F, F\}} \frac{1}{2} \left(\mathbf{v}_q + \frac{\Delta t}{\rho_q} (\nabla_h p)_q \right) - \frac{\Delta t}{\rho_f} (\nabla_h p)_f$$

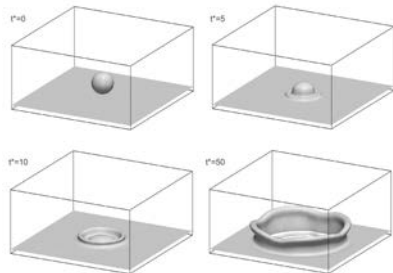
8. Repeat steps 2-7 until to achieve the desired time.

¹ Balcázar et al., (2014). A finite-volume/level-set method for simulating two-phase flows on unstructured grids, Int. J. Multiphase Flow 64, 55-72. <https://doi.org/10.1016/j.ijmultiphaseflow.2014.04.008>

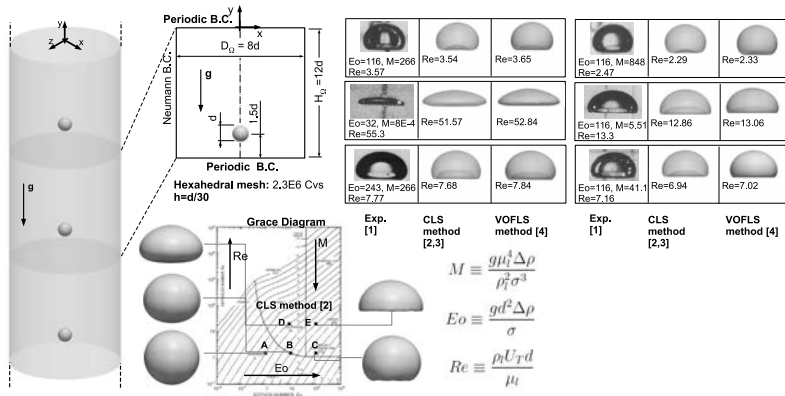
² Balcázar et al., (2016). A level-set model for thermocapillary motion of deformable fluid particles, Int. J. Heat Fluid Flow 62, Part B, 324-343. <http://dx.doi.org/10.1016/j.ijheatfluidflow.2016.09.015>

⁶ Balcázar et al., (2017). DNS of the wall effect on the motion of bubble swarms, Procedia Computer Science 108, 2008-2017. <https://doi.org/10.1016/j.procs.2017.05.076>

- 1 Introduction.
- 2 Mathematical formulation and numerical methods.
- 3 Numerical experiments.**
- 4 Conclusions.

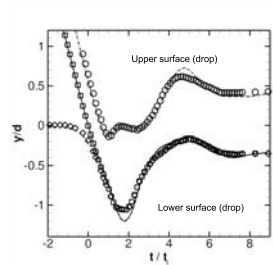
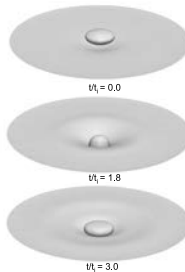
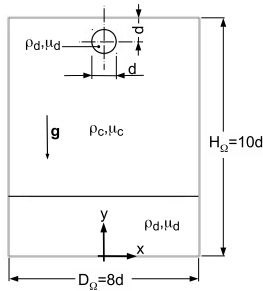


Single buoyant bubbles (Validations) [2, 3, 4]



- [1] Bhaga and Weber (1981), Bubbles in viscous liquids: shapes, wakes and velocities. *Int. J. Multiphase Flow* 33
[2] Balcázar et al. (2014), A finite-volume/level-set method for simulating two-phase flows on unstructured grids, *International Journal of Multiphase Flow* 64, Pages 55-72
[3] Balcázar et al. (2015), Level-set simulations of buoyancy-driven motion of single and multiple bubbles, *International Journal of Heat and Fluid Flow* 56, Pages 91-107
[4] Balcázar et al. (2016), A coupled volume-of-fluid/level-set method for simulation of two-phase flows on unstructured meshes. *Computers and Fluids* 124. Pages 12-29.

Droplet collision against a fluid interface (Validations) [1]



Hexahedral mesh, 5.98×10^6 Cvs, $h = d/30$

$$M \equiv \frac{g \mu_c^4 \Delta \rho}{\rho_c^2 \sigma^3} = 8.82 \times 10^{-8} \quad Eo \equiv \frac{g d^2 \Delta \rho_c}{\sigma} = 6.4$$

$$\eta_\rho \equiv \frac{\rho_c}{\rho_d} = 1.19 \quad \eta_\mu \equiv \frac{\mu_c}{\mu_d} = 0.33$$

Multiple marker CLS method [1]



Experiments reported by [2]



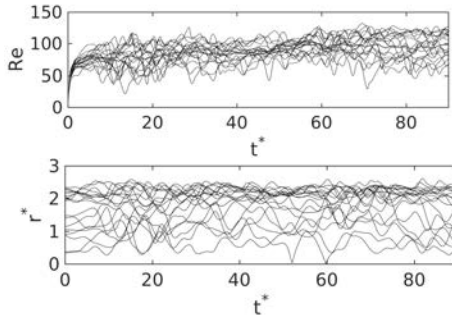
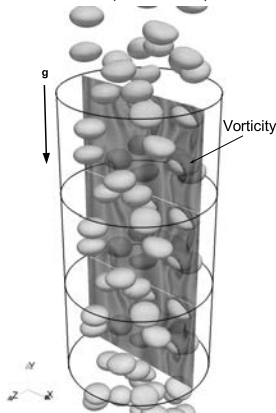
$$1.2 \quad |\mathbf{v} \cdot \mathbf{e}_y| / U_i \quad 0.0$$

[1] Balcázar et al. (2015), Int. J. Multiphase Flow 74, 125-142

[2] Mohamed-Kassim and Longmire (2003), Phys. Fluids 15, 3263-3273

Applications: Gravity-driven bubbly flows [6, 7]

18 bubbles, $Eo = 3$, $Mo = 10^{-6}$, $\eta_\mu = \eta_\rho = \eta_\lambda = 100$. (2086 CPU cores)



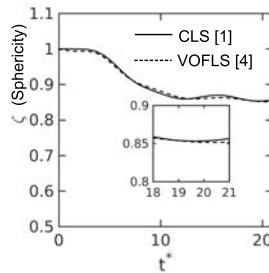
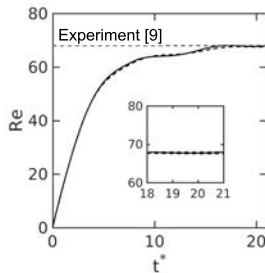
- Deformable bubbles do not touch the wall (wall effect).
- Random fluctuations in Reynolds number (Re) of single bubbles.
- Average Reynolds number (Re) of the swarm tends to steady state.
- Predictive simulations: $Re = Re(Eo, Mo, \text{bubble fraction}, N_b, \text{Conf. Ratio})$.

⁶ Balcázar et al., (2017). DNS of the wall effect on the motion of bubble swarms, Procedia Computer Science 108, 2008-2017. <https://doi.org/10.1016/j.procs.2017.05.076>

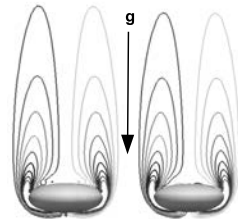
⁷ Balcázar et al., (2018). Direct and Large-Eddy Simulation X. ERCOFTAC Series, vol 24. Springer, Cham. https://doi.org/10.1007/978-3-319-63212-4_15

Falling droplets (Validation) [8]

$Eu = 6.4$, $Mo = 1.03 \times 10^{-5}$, $\eta_\mu = 0.33$, $\eta_\rho = 1.19$, $CR = 8$,
(D_Ω, H_Ω) = ($CR \cdot d, 12d$), $h = d/30$ (4.4MCV s), 256 CPU-cores.



CLS [1] VOFLS [4]



¹ Balcázar et al., (2014). Int. J. Multiphase Flow 64, 55-72.

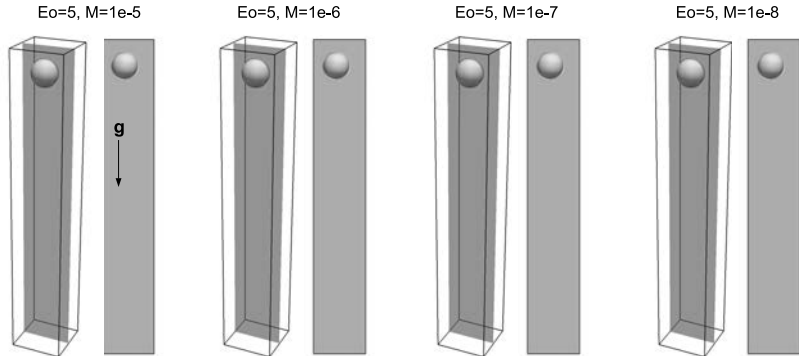
⁴ Balcázar et al., (2016). Computers & Fluids 124, 12-29.

⁸ Balcázar et al., (2018). DNS of Falling Droplets in a Vertical Channel.. International Journal of Computational Methods and Experimental Measurements. Volume 6, Issue 2, pp. 398-410.

⁹ Mohamed-Kassim and Longmire (2003), Phys. Fluids 15, 3263-3273

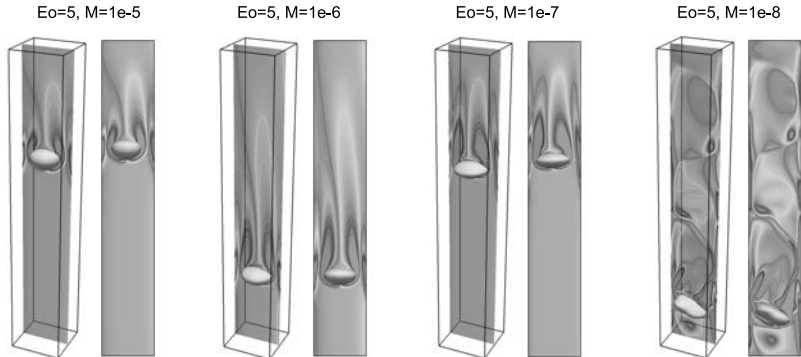
Applications: Falling droplets [8].

Falling droplets at $\eta_\mu = 1.0$, $\eta_p = 1.2$, $CR = 2$, $(D_\Omega, H_\Omega) = (2d, 10d)$ (square channel), $h = d/40$ (3.072M CVs), 128 CPU-cores.



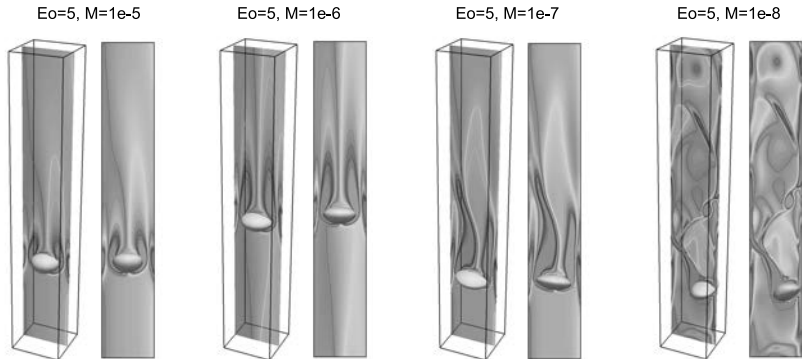
Applications: Falling droplets [8].

Falling droplets at $\eta_\mu = 1.0$, $\eta_\rho = 1.2$, $CR = 2$, $(D_\Omega, H_\Omega) = (2d, 10d)$ (square channels), $h = d/40$ (3.072M CVs), 128 CPU-cores.



Applications: Falling droplets [8].

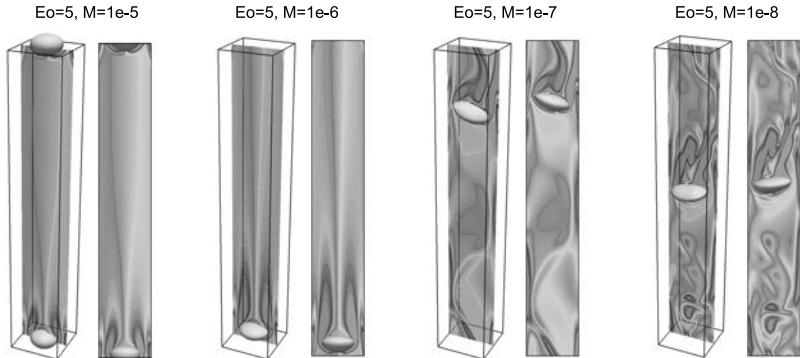
Falling droplets at $\eta_\mu = 1.0$, $\eta_\rho = 1.2$, $CR = 2$, $(D_\Omega, H_\Omega) = (2d, 10d)$ (square channels), $h = d/40$ (3.072M CVs), 128 CPU-cores.



⁸ Balcázar et al., (2018). DNS of Falling Droplets in a Vertical Channel.. International Journal of Computational Methods and Experimental Measurements. Volume 6, Issue 2; pp. 398-410.

Applications: Falling droplets [8].

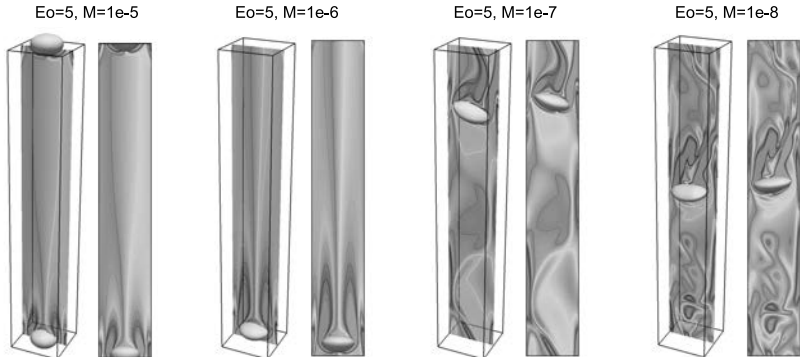
Falling droplets at $\eta_\mu = 1.0$, $\eta_\rho = 1.2$, $CR = 2$, $(D_\Omega, H_\Omega) = (2d, 10d)$ (square channels), $h = d/40$ (3.072M CVs), 128 CPU-cores.



⁸ Balcázar et al., (2018). DNS of Falling Droplets in a Vertical Channel.. International Journal of Computational Methods and Experimental Measurements. Volume 6, Issue 2, pp. 398-410.

Applications: Falling droplets [8].

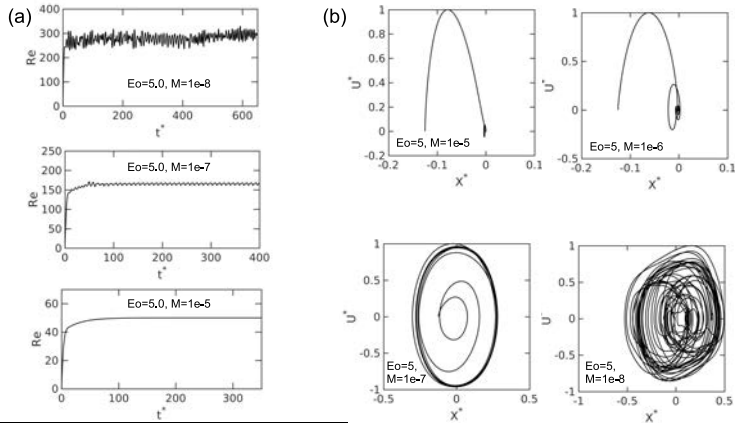
Falling droplets at $\eta_\mu = 1.0$, $\eta_\rho = 1.2$, $CR = 2$, $(D_\Omega, H_\Omega) = (2d, 10d)$ (square channels), $h = d/40$ (3.072M CVs), 128 CPU-cores.



⁸ Balcázar et al., (2018). DNS of Falling Droplets in a Vertical Channel.. International Journal of Computational Methods and Experimental Measurements. Volume 6, Issue 2, pp. 398-410.

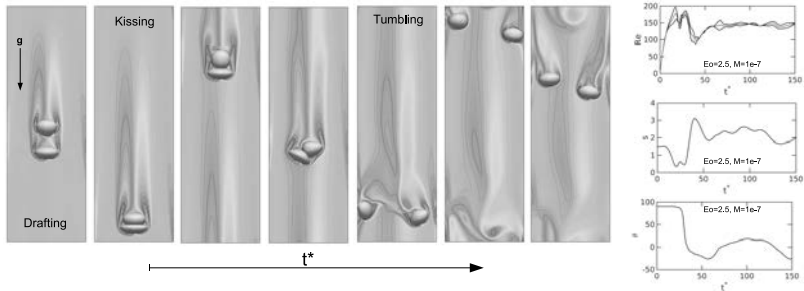
Applications: Falling droplets [8].

Falling droplets at $\eta_\mu = 1.0$, $\eta_\rho = 1.2$, $CR = 2$, $(D_\Omega, H_\Omega) = (2d, 10d)$ (square channels), $h = d/40$ (3.072M CVs), 128 CPU-cores.

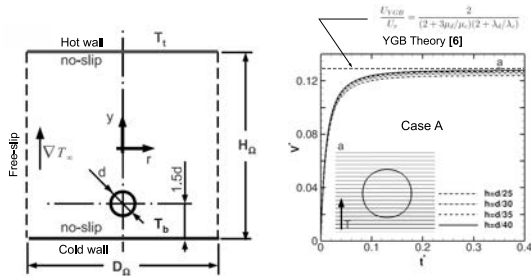


Applications: Interaction of 2 falling droplets [8].

2 droplets at $Eo = 2.5$, $Mo = 10^{-7}$, $\eta_\mu = 1.0$, $\eta_\rho = 1.2$, $CR = 4$,
(D_Ω, H_Ω) = ($4d, 10d$) (square channels), $h = d/40$ (12.288M CVs), 512
CPU-cores.

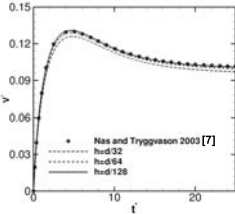


Thermocapillary motion of single droplets ($g=0$) [5]



$$Re = 5, Ma = 20, Ca = 0.01$$

$$= \eta_\mu = \eta_{c,p} = \eta_\lambda = 0.5$$

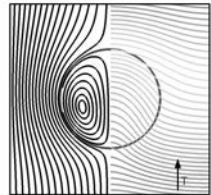


$$Ma = \frac{\sigma_T ||\nabla T_\infty|| d^2 \rho_c c_{p,c}}{4\mu_c \lambda_c} \quad Re = \frac{\sigma_T ||\nabla T_\infty|| d^2 \rho_c}{4\mu_c^2} \quad Ca = \frac{\sigma_T ||\nabla T_\infty|| d}{2\sigma_0}$$

$$U_r = \sigma_T ||\nabla T_\infty|| (d/2)/\mu_c \quad t^* = 2tU_r/d \quad V^* = (\mathbf{e}_y \cdot \mathbf{v}_c)/U_r$$

Re	Ca	Ma	η_μ	η_μ	η_λ	$\eta_{c,p}$	U_{YGB}/U_r	$(U/U_r)_{num}$
0.066	0.066	0.066	1.0	1.0	1.0	1.0	0.133	0.128

Ma_{sch}	(D_c, H_c)	C_{colle}	C_{colle}/n_{lane}	N_c	$C_{colle}/n_{hexagonal}$	$h/d/40$
4	(80, 80)	4.09×10^{-7}	12800	320		



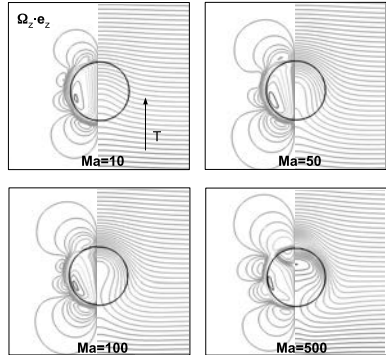
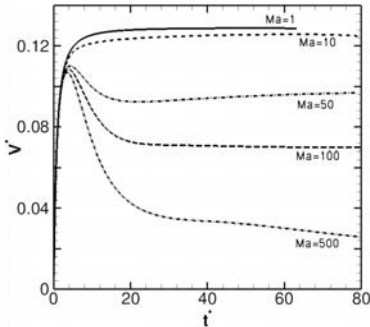
[6] Young, N. O., Goldstein, J. S., Block, M. J. (1959). The motion of bubbles in a vertical temperature gradient. J. Fluid Mech. 6, 350-356.

[7] S. Nas, G. Tryggvason, Thermocapillary interaction of two bubbles or drops, Int. J. Multiphase Flow 29 (2003) 1117-1135.

[5] Balcázar et al. (2016), A level-set model for thermocapillary motion of deformable fluid particles, Int. J. Heat and Fluid Flow 62, 324-343.

Thermocapillary motion of single droplets ($g=0$) [5]

$Re=5$, $Ca=0.1$, $\eta\rho=\eta_\mu=\eta_{cp}=\eta_\lambda=1.0$



$$Ma = \frac{\sigma_T \|\nabla T_\infty\| d^2 \rho_c c_{p,c}}{4\mu_c \lambda_c}$$

$$Re = \frac{\sigma_T \|\nabla T_\infty\| d^2 \rho_c}{4\mu_c^2}$$

$$Ca = \frac{\sigma_T \|\nabla T_\infty\| d}{2\sigma_0}$$

$$U_r = \sigma_T \|\nabla T_\infty\| (d/2) / \mu_c$$

$$t^* = 2tU_r/d$$

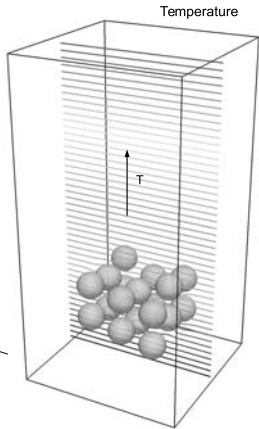
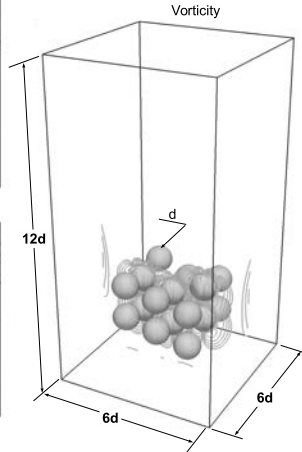
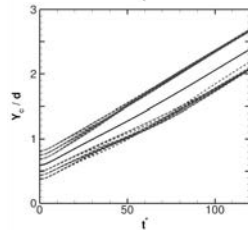
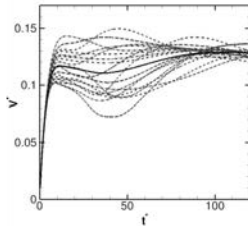
$$V^* = (\mathbf{e}_y \cdot \mathbf{v}_c) / U_r$$

[5] Balcázar et al. (2016), A level-set model for thermocapillary motion of deformable fluid particles, *Int. J. Heat and Fluid Flow* 62, 324–343.

Thermocapillary interaction of multiple droplets ($g=0$)

18 droplets: $Re=40$, $Ma=40$, $Ca=0.04166$, $\eta_p=\eta_u=\eta_{cp}=\eta_\lambda=0.5$

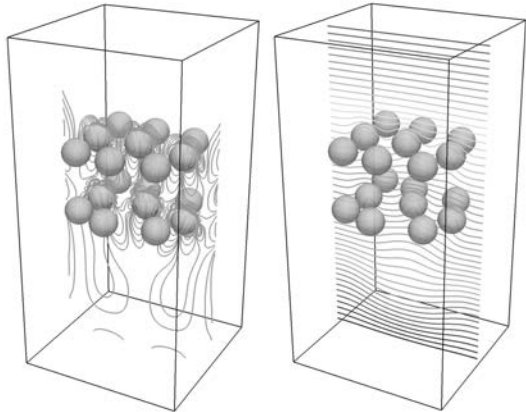
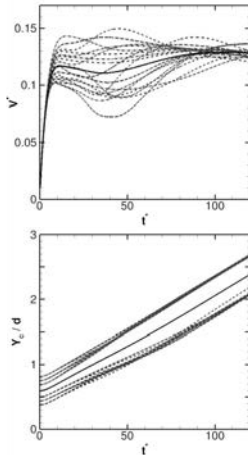
Mesh: cartesian $240 \times 240 \times 480$, $h=d/40$, 1024 CPU cores



Thermocapillary interaction of multiple droplets ($g=0$)

18 droplets: $Re=40$, $Ma=40$, $Ca=0.04166$, $\eta_p=\eta_\mu=\eta_{cp}=\eta_\kappa=0.5$

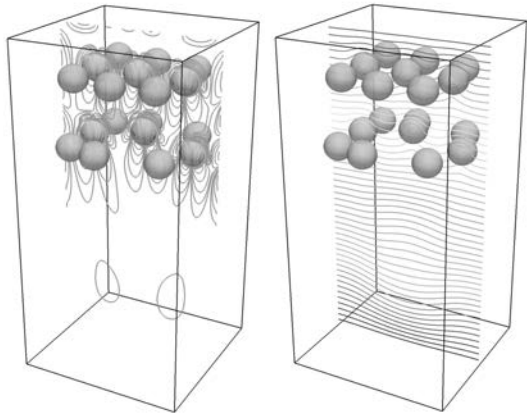
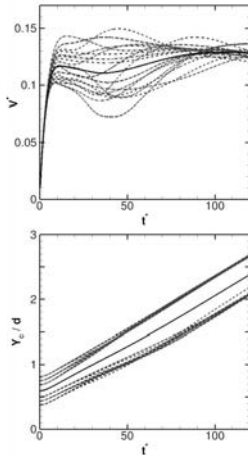
Mesh: cartesian 240x240x480, $h=d/40$



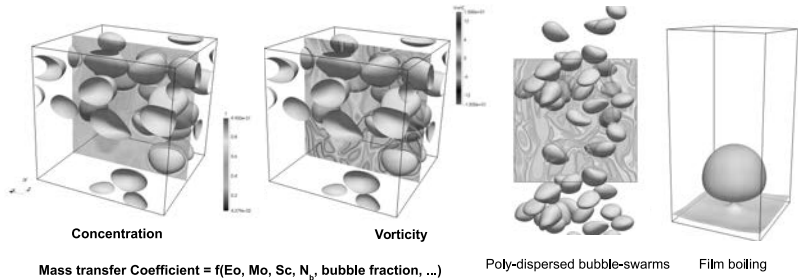
Thermocapillary interaction of multiple droplets ($g=0$)

18 droplets: $Re=40$, $Ma=40$, $Ca=0.04166$, $\eta_p=\eta_\mu=\eta_{cp}=\eta_\lambda=0.5$

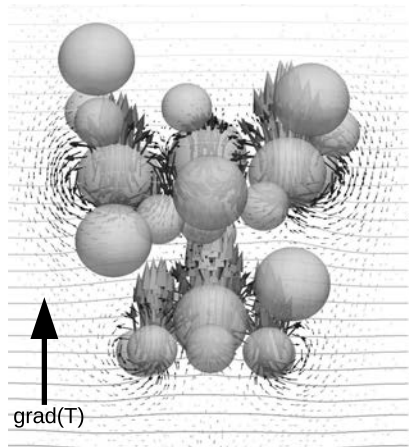
Mesh: cartesian 240x240x480, $h=d/40$



Ongoing work: More details in [9]



- 1 Introduction.
- 2 Mathematical formulation and numerical methods.
- 3 Numerical experiments.
- 4 Conclusions.**



- Mass conservative interface capturing methods have been introduced for simulation of two-phase flows on 3D unstructured meshes, including surface tension effects.
- A multiple marker interface capturing method has been introduced for simulation of bubble swarms.
- These methods have been extensively validated and verified against experiments, analytical and numerical results from the literature.
- Current work extends the capabilities of these solvers to interfacial heat and mass transfer, variable surface tension (e.g. Thermocapillary effects).
- Future work includes extension of these capabilities to phase-change phenomena and surfactant effects.

Acknowledgements

- This work has been financially supported by the *Ministerio de Economía y Competitividad, Secretaría de Estado de Investigación, Desarrollo e Innovación* (MINECO), Spain (ENE2015-70672-P) and Termo Fluids S.L.
- Néstor Balcázar acknowledges financial support of the *Programa Torres Quevedo* (PTQ-14-07186) MINECO, Spain.
- Part of 3D simulations of these works have been performed using computing time provided by PRACE 10th-Call (Ref: 2014112666) and PRACE 14th-Call (Ref. 2016153612) at supercomputer MareNostrum III and IV, based in Barcelona, Spain.